



**Repositorio Institucional de la Universidad Autónoma de Madrid**

<https://repositorio.uam.es>

Esta es la **versión de autor** del artículo publicado en:

This is an **author produced version** of a paper published in:

Theoretical Chemistry Accounts 138.4 (2019): 59

**DOI:** <https://doi.org/10.1007/s00214-019-2451-0>

**Copyright:** © Springer-Verlag GmbH Germany, part of Springer Nature 2019

El acceso a la versión del editor puede requerir la suscripción del recurso

Access to the published version may require subscription

# Role of Intramolecular Hydrogen Bonds and Electron Withdrawing Groups in the Acidity of Aldimines and Ketimines: a Density Functional Theory Study

Fernando Aguilar-Galindo<sup>1</sup>, Ana María Tuñón<sup>1</sup>, Alberto Fraile<sup>2,3</sup>, José Alemán<sup>2,3</sup>, Sergio Díaz-Tendero<sup>1,3,4,\*</sup>

<sup>1</sup>Departamento de Química, Universidad Autónoma de Madrid, 28049 Madrid, Spain

<sup>2</sup>Departamento de Química, Orgánica, Universidad Autónoma de Madrid, 28049 Madrid, Spain

<sup>3</sup>Institute for Advanced Research in Chemical Sciences (IAdChem), Universidad Autónoma de Madrid, 28049 Madrid, Spain

<sup>4</sup>Condensed Matter Physics Center (IFIMAC), Universidad Autónoma de Madrid, 28049 Madrid, Spain

\* [sergio.diaztendero@uam.es](mailto:sergio.diaztendero@uam.es)

**Abstract** The role of intramolecular hydrogen bonds and the presence of electron withdrawing groups in the acidity of secondary aldimines and secondary ketimines is investigated by means of density functional theory simulations. We have found that the presence of an intramolecular hydrogen bond can increase the acidity up to  $\sim 20 \text{ kJ}\cdot\text{mol}^{-1}$  with respect to structural isomers not showing it. In general, the excess of negative charge in the deprotonated species is hosted by the electron withdrawing group, thus stabilizing the anion and increasing the acidity. Among the studied structures, secondary ketimines, bearing a phenyl group, have shown to present the lowest acidity, and are therefore potential candidates that would be used for different Michael and nucleophilic additions in the synthesis of important pharmaceutical and natural products.

## Introduction

Hydrogen bond represents one of the most relevant chemical bonding forces in nature. The structure of proteins and the famous shape of DNA is driven by this important, although weak, interaction. The energy of the hydrogen bond is between 1 and 40  $\text{kcal}\cdot\text{mol}^{-1}$ ,<sup>1</sup> therefore it shows a strength between a covalent bond and a van der Waals interaction.<sup>2</sup> Within catalysis, and more specifically, in organocatalysis, hydrogen bonding has played a crucial role in different types of catalysts, such as squaramides,<sup>3</sup> thioureas,<sup>4</sup> or TADDOL ( $\alpha,\alpha,\alpha',\alpha'$ -tetraaryl-2,2-disubstituted 1,3-dioxolane-4,5-dimethanol).<sup>5</sup> Therefore, intermolecular hydrogen bond interaction between the catalyst and substrates has been deeply studied. However, intramolecular hydrogen bond activation of nucleophiles or electrophiles has been much less explored.

In the case of activation of electrophiles, many papers have been published, such as activation of ketones from the Palomo's group,<sup>6</sup> nitroalkenes from the Vicario's group,<sup>7</sup> aldehydes by Jung and Krische<sup>8</sup> or  $\alpha$ ,  $\beta$  amides-unsaturated derivatives of Takemoto et al.<sup>9</sup> (top, Scheme 1). However, until very recently, there were no organocatalytic examples that would have used nucleophilic activation by hydrogen bonding. Da's group presented in 2017<sup>10</sup> intramolecular hydrogen bond activation of ketones, using a hydroxyl group (bottom, Scheme 1). A few months later, we published the use of phenols derived for the intramolecular activation of different nucleophiles. Specifically, we were able to activate azamethylene imines to obtain pyrrolidines<sup>11</sup> and amino acid derivatives.<sup>12</sup> In addition, we were also able to increase the acidity of an imine derivative to achieve aza-Michael reactions to  $\alpha,\beta$ -unsaturated aldehydes<sup>13</sup> (bottom, Scheme 1). We found that, in these reactions, not only the transition states (TS) were important, but also that the pre-association stage of the formed complexes (PAC)<sup>14</sup> was critical for the preorganization of the TS.<sup>15</sup> In the search for new reactions, and for so many new activations by hydrogen bonding, we ask ourselves, if we would be able to find activations of other substrates by intramolecular hydrogen bond. In this work, we propose the search for new substrates for activation by intramolecular hydrogen bond and studied their acidity using density functional theory simulations. In particular we focus on the secondary aldimines and secondary ketimines presented in Fig.1; structures showing different electron withdrawing groups.

### Computational Details

All calculations were performed in the frame of the Density Functional Theory (DFT) with the Gaussian09 (E.01 revision)<sup>16</sup>. The Minnesota M06-2X exchange-correlation functional<sup>17</sup> has been chosen for this study due to its capability to correctly reproduce non-covalent interactions in organic molecules (see e.g.<sup>18-20</sup>). In order to describe in a proper way intramolecular hydrogen bonds and electron density in anionic species, we have used the 6-31++G(d,p) Pople's basis set, which contains diffuse functions, both in the hydrogens and in the heavy atoms, that are required for this kind of systems. Stationary points obtained in the geometry optimization, were confirmed to be minima of the Potential Energy Surface (PES) through the corresponding frequency analysis by checking that they do not present imaginary frequencies. In order to determine the distribution of the electron density, Natural Bond Orbitals (NBO)<sup>21</sup> were obtained on the top of the optimized structures to obtain the natural charges through a Natural Population Analysis (NPA), which is less basis-dependent than the Mulliken ones, using the NBO3.1

code<sup>22</sup>. Hydrogen bonds were characterized using the Quantum Theory of Atoms-In-Molecules (QT-AIM)<sup>23-24</sup> with the AIMAll code<sup>25</sup>.

## Results and Discussion

In order to study the effect of different intramolecular hydrogen bonds on the acidity, we have selected the five base structures shown in Fig. 1a. We have changed six different Electron Withdrawing Groups (EWG) on these molecular skeletons (Fig. 1b), thus checking their effect in the acidity as well. In the geometry optimization of the neutral species we have considered the rotamers that, a priori, are non-equivalent; for the anionic conjugated species we considered the cis-trans geometries with respect to the formally double N=C bond. Combination of the 5 base molecules with the 6 EWG and taking 2 different conformers in each case provides a total of 120 structures (60 neutral and the corresponding 60 anions). A summary of the relative energy between them is given in the appendix.

Figs. 2-6 show the most stable conformation of both, neutral and anionic forms in structures **A-E**, with the different considered EWGs. As expected, anions tend to be arranged in a trans configuration with respect to the N-C bond which, due to conjugation with the C=N bond, acquires a partial double bond character. In those cases where the EWG is able to delocalize electron density through mesomeric effect, the withdrawing group tends to be arranged in the same plane to stabilize the negative charge by delocalization.

In the case of neutral molecules, no clear trends are observed in the geometry. Since the CH<sub>2</sub>-EWG bond has free rotation and there is no conjugation, the relative stability is mainly established due to steric effects and non-covalent interactions.

The most stable geometry for each specie has been used to compute deprotonation free energies in the gas phase. To this we used the correction of the free energy of the proton (0.01 a.u., see<sup>26</sup> for further details). In order to illustrate the observed trends, we have represented the computed values by grouping molecules with the same base structure **A-E** (see Fig.7).

Comparing results for molecular skeletons **A**, **B** and **C**, we observe lowering in  $\Delta G$  for structures **B**; higher stabilization of the anionic form due to the presence of the thiocarboxylic group reduces the required energy to deprotonate the molecule. Among these three sets of molecules, those with an amide group, **C**, show higher  $\Delta G$ , i.e. lower stabilization of the anion. This was expected since the amide group has a weaker



mesomeric effect. Structure **D** is similar to structure **A-Ph**, but with an extra EWG. This group stabilizes the conjugate anionic base and thus, deprotonation energies are lower. In particular structure **D-CN** shows a very low  $\Delta G$ . Finally, deprotonation of **E**-derivatives requires, in general, higher energy. The functional group of the base structure (phenol) is a ring with high electron density and with lower capacity to delocalize negative charge of the anion efficiently, thus decreasing the acidity.

In general, EWGs that combine mesomeric effects with presence of groups with highly electronegative heteroatoms, attract the electronic density more efficiently therefore stabilizing the anion form and increasing the acidity (-COPh, -CN, -CO<sub>2</sub>Me). In the case of amide, -CONMe<sub>2</sub>, which also combines mesomeric effect with electronegative heteroatoms, the effect is weaker than in the ester -CO<sub>2</sub>Me, because the electron pair of the nitrogen atom counteracts the mesomeric effect. For the -CF<sub>3</sub> group only electron attractive -I effect is present, and for -Ph group electron delocalization is barely stabilized in the C atoms of the ring, thus showing smaller anionic stabilization and lower acidity among the considered substituted species.

In order to determine the effect of the EWG, we have computed deprotonation energies of the base structures **A-E** without withdrawing group (i.e. EWG=H). The obtained results, also presented in Fig.7 for comparison, show larger  $\Delta G$  in each set of data, pointing out the clear effect of the EWGs in stabilizing negative charge in the conjugate anion.

All base structures, in their most stable conformer, exhibit an intramolecular hydrogen bond, in both neutral and anionic form. But, does this interaction play a role in the acidity of these compounds? To shed light on this question we have considered alternative structures without EWG and with the H pointing towards the opposite direction. In this way, all mesomeric effects remains constant and we can focus only in this particular interaction. Scheme 2 shows the results obtained in both configurations (with and without H bond) for structures **A-E** without EWG. Molecule **C** (the amide one) is not shown, since a rotation of 180° of the C-N bond provides an equivalent structure keeping the hydrogen bond.

In the case of the structures **A**, **D** and **E** the presence of the hydrogen bond increases the acidity of the molecule. This effect is especially important in the case of structure **E**, where a 6-member ring is formed with the H-bond and thus a lower deformation energy is required for this interaction. For structure **B** the hydrogen bond stabilizes both neutral and anionic forms of the molecule, but the protonated one in a much higher degree. As

a consequence of the much stronger H bond in the neutral form of structure **B**, the intrinsic acidity is lower with the presence of the hydrogen bond. To show this, we have analyzed the vibrational frequency of the O-H stretching mode ( $\nu_{\text{OH}}$ ) in base structures **A** and **B**, with and without hydrogen bond, in both neutral and anionic forms. These results are shown in Table 1. In the two cases changes in the  $\nu_{\text{OH}}$  frequency due to deprotonation in absence of hydrogen bond is similar,  $\sim 30 \text{ cm}^{-1}$  higher in the anionic forms. This change is due to the different electron density in this part of the molecule. On the other hand, if hydrogen bond is present, this IR band redshifts much more from neutral to anionic species in structure **B** ( $43 \text{ cm}^{-1}$ ). Therefore, it seems to indicate that the intramolecular hydrogen bond in structure **B** behaves differently than in the other structures, being responsible for the changes observed in acidity. In order to confirm this hypothesis, we have evaluated the strength of the hydrogen bond by computing the density in the bond critical point (BCP).

The results (see Fig. 8) show that the electronic density at the BCP of the hydrogen bond increases with the deprotonation in structures **A** (13%) **D** (11%) and **E** (19 %), thus making this bond stronger and stabilizing the corresponding anionic species. However, the electron density in the BCP of the hydrogen bond in structure **B** decreases slightly in the anionic form ( $\sim 1\%$ ), pointing out a stronger intramolecular interaction in the neutral form of structure **B**, unlike other cases. This explains observed changes in the acidity with the hydrogen bond. But, why structure **B** does not increase the stability of the hydrogen bond after deprotonation as other structures do? The reason is easily found by analyzing the change in strength in surrounding bonds: The electron density in the BCP of C=O bond in **A** and **D** is reduced in  $\sim 6$  and  $\sim 5\%$  respectively, while for C=S bond in **B** is reduced in more than 10%. Thus, different charge reorganization in these structures with the deprotonation causes a larger stabilization of anionic structures **A**, **D** and **E**, thus increasing the acidity, and on the contrary stabilizing the neutral form of structure **B** to a greater extent and thus decreasing the acidity.

We have also analyzed the effect of the EWG in hosting the excess of negative charge in deprotonated species and how it affects the acidity. Fig. 9 shows deprotonation Gibbs free energies as a function of the charge located on atoms of the EWG in the anionic species,  $Q_{\text{EWG}}$ . As a general trend we observe decrease in  $\Delta G$  with  $Q_{\text{EWG}}$ , i.e. stabilization of the excess of charge by the EWG increases the acidity. Results in **D** and **E** are more scattered, probably due to the presence of a phenyl group that might help in the electron delocalization and thus stabilization of the charge is not only due to the presence of an EWG but in the whole structure.

Since the effect of the solvent can modify intramolecular interactions, we have also calculated deprotonation Gibbs free energies ( $\Delta G$ ) by including solvent effects, by using the Polarizable Continuum Model (PCM) through the SMD formalism.<sup>27</sup> In particular we employed the methodology developed by Markovic and coworkers<sup>28,29</sup> to include the solvent molecules in the deprotonation. This method has been proven to be efficient in other types of systems<sup>30</sup>. Fig.10 shows deprotonation  $\Delta G$  using *p*-xylene and THF, widely used solvents. We observe that (i) including solvent effects increases the acidity because the proton is stabilized by the presence of solvent molecules and (ii) in the case of THF the increase is higher than in *p*-xylene because the former is more polar and because it has a basic center (an oxygen atom) where the proton can be accommodated.

## Conclusions

In this work we have studied the acidity of secondary aldimines and secondary ketimines using the density functional theory. We have focused on structures showing intramolecular hydrogen bonds and with different electron withdrawing groups (EWGs). We have demonstrated that the charge hosted by the EWG stabilizes anionic forms and therefore increases the acidity. The presence of a hydrogen bond also increases the acidity. Among the studied species, secondary ketimines bearing a phenyl group (in particular structures **D-CN** and **D-CF<sub>3</sub>**) present the highest acidity, thus showing as promising candidates for future reactivity studies. In the case of organocatalyzed reactions, one has to consider that the energetic profile of the reaction will be strongly modified by the interaction between catalyst and reagents, through the formation of pre-association complexes, as we have previously shown<sup>14,15</sup>.

## Acknowledgments

The authors acknowledge the generous allocation of computer time at the Centro de Computación Científica of the Universidad Autónoma de Madrid (CCC-UAM). This work was partially supported by the projects CTQ2016-76061-P & CTQ2015-64561-R of the Spanish Ministerio de Economía y Competitividad (MINECO). F.A.G. acknowledges the FPI grant associated with the project CTQ2013-43698-P (MINECO). Financial support from the MINECO through the “María de Maeztu” Program for Units of Excellence in R&D (MDM-2014-0377) is also acknowledged.

## References

1. Jeffrey GA (1997) An Introduction to Hydrogen Bonding, Oxford University Press.

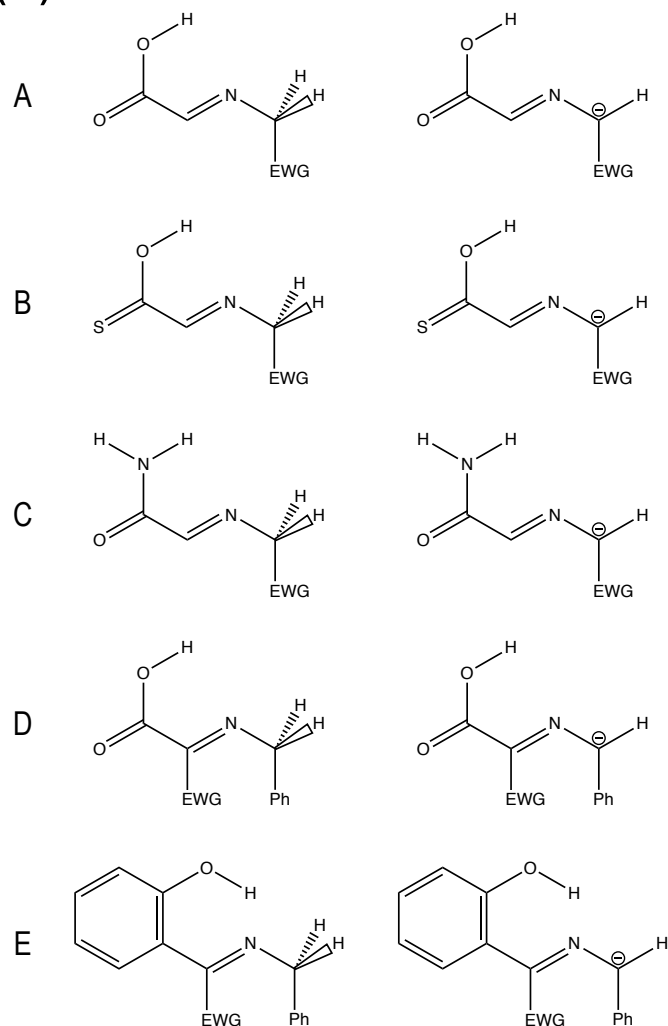
2. Steiner T (2002) The Hydrogen Bond in the Solid State. *Angew Chem Int Ed* 41(1): 48-76 [https://doi.org/10.1002/1521-3773\(20020104\)41:1<48::AID-ANIE48>3.0.CO;2-U](https://doi.org/10.1002/1521-3773(20020104)41:1<48::AID-ANIE48>3.0.CO;2-U)
3. Aleman J, Parra A, Jiang H, Jorgensen KA (2011) Squaramides: Bridging from Molecular Recognition to Bifunctional Organocatalysis. *Chem Eur J* 17(25): 6890-6899 <https://doi.org/10.1002/chem.201003694>
4. Zhang Z, Schreiner PR (2009) (Thio)urea organocatalysis-What can be learnt from anion recognition? *Chem Soc Rev* 38: 1187-1198 <https://doi.org/10.1039/B801793J>
5. Huang Y, Unni AK, Thadani AN, Rawal VH (2003) Single enantiomers from a chiral-alcohol catalyst. *Nature* 424: 146 <https://doi.org/10.1038/424146a>
6. Badiola E, Fiser B, Gómez-Bengoña E, Mielgo A, Olaizola I, Urruzuno I, García JM, Odriozola JM, Razkin J, Oirabide M, Palomo C (2014) Enantioselective Construction of Tetrasubstituted Stereogenic Carbons through Brønsted Base Catalyzed Michael Reactions:  $\alpha'$ -Hydroxy Enones as Key Enolate Equivalent. *J Am Chem Soc* 136(51): 17869-177881 <https://doi.org/10.1021/ja510603w>
7. Talavera G, Reyes E, Vicario JL, Carrillo L (2012) Cooperative Dienamine/Hydrogen-Bonding Catalysis: Enantioselective Formal [2+2] Cycloaddition of Enals with Nitroalkenes. *Angew Chem Int Ed* 51(17): 4104-4107 <https://doi.org/10.1002/anie.201200269>
8. Jung CK, Krische MJ (2006) Asymmetric Induction in Hydrogen-Mediated Reductive Aldol Additions to  $\alpha$ -Amino Aldehydes Catalyzed by Rhodium: Selective Formation of syn-Stereotriads Directed by Intramolecular Hydrogen-Bonding. *J Am Chem Soc* 128(51): 17051-17056 <https://doi.org/10.1021/ja066198q>
9. Inokuma T, Hoashi Y, Takemoto Y (2006) Thiourea-Catalyzed Asymmetric Michael Addition of Activated Methylene Compounds to  $\alpha,\beta$ -Unsaturated Imides: Dual Activation of Imide by Intra- and Intermolecular Hydrogen Bonding. *J Am Chem Soc* 128(29): 9413-9419 <https://doi.org/10.1021/ja061364f>
10. Wang P, Li HF, Zhao JZ, Du, ZH, Da CS (2017) Organocatalytic Enantioselective Cross-Aldol Reaction of  $\alpha$ -Hydroxyarylketones and Trifluoromethyl Ketones. *Org Lett* 19(10): 2634-2637 <https://doi.org/10.1021/acs.orglett.7b00828>
11. Esteban F, Cieslik W, Arpa EM, Guerrero-Corella A, Díaz-Tendero S, Perles J, Fernández-Salas JA, Fraile A, Alemán J (2018) Intramolecular Hydrogen Bond Activation: Thiourea- Organocatalyzed Enantioselective 1,3-Dipolar Cycloaddition of Salicylaldehyde-Derived Azomethine Ylides with Nitroalkenes. *ACS Catal* 8(3):1884-1890, <https://doi.org/10.1021/acscatal.7b03553>
12. Guerrero-Corella A, Esteban F, Iniesta M, Martín-Somer A, Parra M, Díaz-Tendero S, Fraile A, Alemán J (2018) 2-Hydroxybenzophenone as Chemical Auxiliary for the Activation of Ketiminoesters in the Highly Enantioselective Addition to Nitroalkenes under Bifunctional Catalysis. *Angew Chem Int Ed* 57(19): 5350-5354, <https://doi.org/10.1002/anie.201800435>

13. Choubane H, Garrido-Castro AF, Alvarado C, Martín-Somer A, Guerrero-Corella A, Daaou M, Díaz-Tendero S, Maestro MC, Fraile A, Alemán A (2018) Intramolecular hydrogen-bond activation for the addition of nucleophilic imines: 2-hydroxybenzophenone as a chemical auxiliary. *Chem Commun* 54: 3399-3402 <https://doi.org/10.1039/C8CC01479E>
14. Arpa EM, Frías M, Alvarado C, Alemán J, Díaz-Tendero S (2016) Weakly bonded intermediates as a previous step towards highly enantioselectivity iminium type additions of beta-keto-sulfoxides and sulfones. *J Mol Catal A Chem* 423: 308-318, <http://dx.doi.org/10.1016/j.molcata.2016.03.013>
15. Martín-Sómer A, Arpa EM, Díaz-Tendero S, Alemán J (2018) A Density Functional Theory Study of Intramolecular Hydrogen Bond Activation of Aza-Methylene Imines in Hydrogen Bond Bifunctional Catalysis. *Eur J Org Chem* <https://doi.org/10.1002/ejoc.201801208>
16. Frisch et al., Gaussian 09, Revision E.01, Gaussian, Inc., Wallingford CT, 2013.
17. Zhao Y, Truhlar DG (2008) The M06 suite of density functionals for main group thermochemistry, thermochemical kinetics, noncovalent interactions, excited states, and transition elements: two new functionals and systematic testing of four M06-class functionals and 12 other functionals. *Theor Chem Acc* 120(1-3): 215-241 <https://doi.org/10.1007/s00214-007-0310-x>
18. Hohenstein EG, Chill ST, Sherrill D (2008) Assessment of the Performance of the M05-2X and M06-2X Exchange-Correlation Functionals for Noncovalent Interactions in Biomolecules. *J Chem Theory Comput* 4(12):1996-2000 <https://doi.org/10.1021/ct800308k>
19. Thanthirwatte KS, Hohenstein EG, Burns LA, Sherrill CD (2011) Assessment of the Performance of DFT and DFT-D Methods for Describing Distance Dependence of Hydrogen-Bonded Interactions. *J Chem Theory Comput* 7(1):88-96 <https://doi.org/10.1021/ct100469b>
20. Walker M, Harvey AJA, Sen A, Dessent CEH (2013) Performance of M06, M06-2X, and M06-HF Density Functionals for Conformationally Flexible Anionic Clusters: M06 Functionals Perform Better than B3LYP for a Model System with Dispersion and Ionic Hydrogen-Bonding Interactions. *J Phys Chem A* 117(47):12590-12600 <https://doi.org/10.1021/jp408166m>
21. Foster JP, Weinhold F (1980) Natural hybrid orbitals *J. Am. Chem. Soc.*, 102(24): 7211-7218 <https://doi.org/10.1021/ja00544a007>
22. NBO Version 3.1, E. D. Glendening, A. E. Reed, J. E. Carpenter, and F. Weinhold.
23. Bader RFW (1990) *Atoms in Molecules: A Quantum Theory*. Clarendon Press, Oxford, England.
24. Bader RFW (1991) *A Quantum Theory of Molecular Structure and its Applications*. *Chem Rev* 91(5):893-928 <https://doi.org/10.1021/cr00005a013>

25. AIMAll (Version 17.11.14), Todd A. Keith, TK Gristmill Software, Overland Park KS, USA, 2017 (aim.tkgristmill.com).
26. Fife JJ, Dhaouadi Z and Nsangou M (2014) Revision of the Thermodynamics of the Proton in Gas Phase. *J Phys Chem A* 118(46): 11090–11097  
<https://doi.org/10.1021/jp508968z>
27. Marenich AV, Cramer CJ and Truhlar DG (2009) Universal solvation model based on solute electron density and a continuum model of the solvent defined by the bulk dielectric constant and atomic surface tensions. *J Phys Chem B* 113: 6378-96  
<https://doi.org/10.1021/jp810292n>
28. Tosovic J, Markovic S, Milenkovic D and Markovic Z (2016) Solvation Enthalpies and Gibbs Energies of the Proton and Electron – Influence of Solvation Models. *J Serb Soc Comp Mech* 10: 66-76 <https://doi.org/10.5937/jsscm1602066T>
29. Markovic Z, Tosovic J, Milenkovic D, Markovic S (2016) Revisiting the solvation enthalpies and free energies of the proton and electron in various solvents. *Comput Theor Chem* 1077: 11-17 <https://doi.org/10.1016/j.comptc.2015.09.007>
30. Aguilar-Galindo F, Ocón P, Poyato JML (2017) Exploring the catalytic efficiency of X-doped (X=B, N, P) graphene in oxygen reduction reaction: Influence of solvent and border effects. *Int J Quantum Chem*. 118:e25579 <https://doi.org/10.1002/qua.25579>

## Schemes, Figures and Tables

(a)



(b)

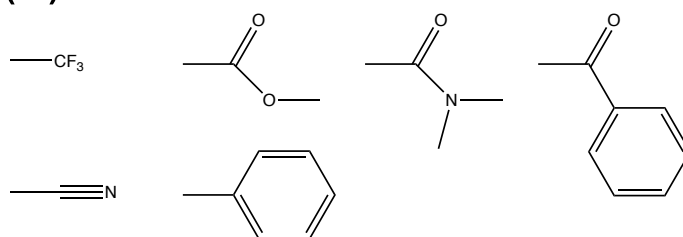


**Figure 1:** (a) Molecular structures considered in this work (A-E); the left column shows neutral structures and the right column the deprotonated anionic ones. (b) Electron withdrawing groups substituted in the molecular structures.

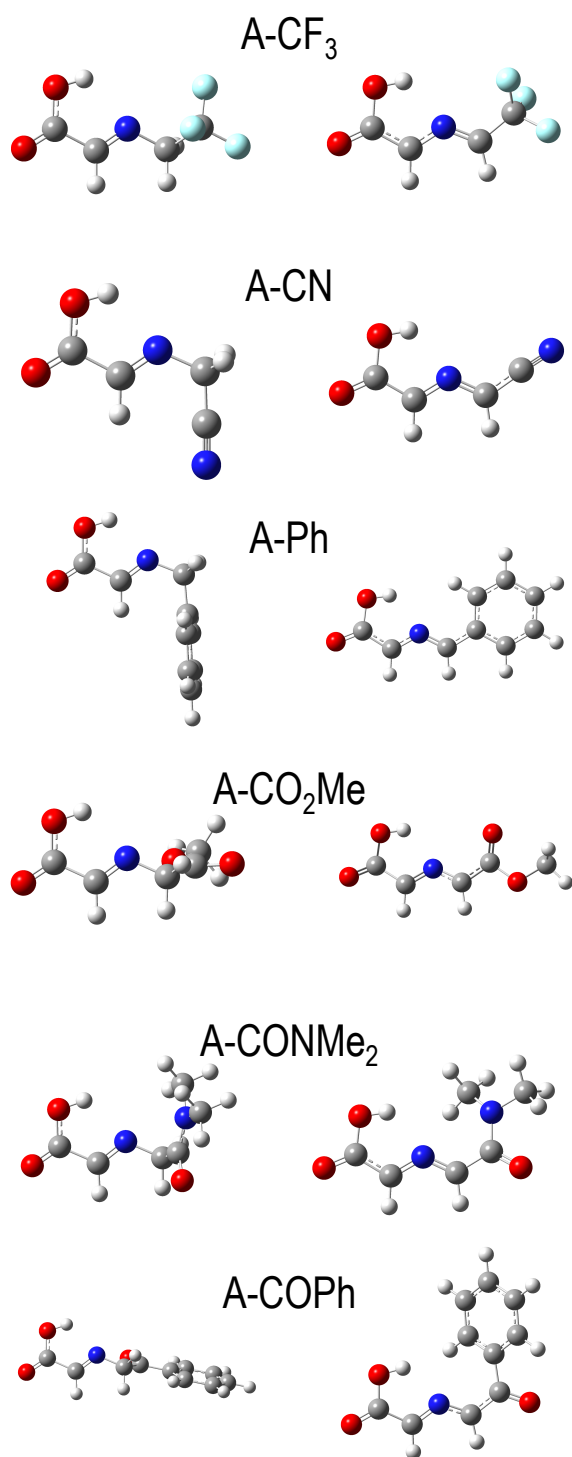


**Figure 2:** Most stable isomers of molecular structure **A** with the different EWG studied (see Fig.1). Left column neutral structures, right column anionic counterparts.



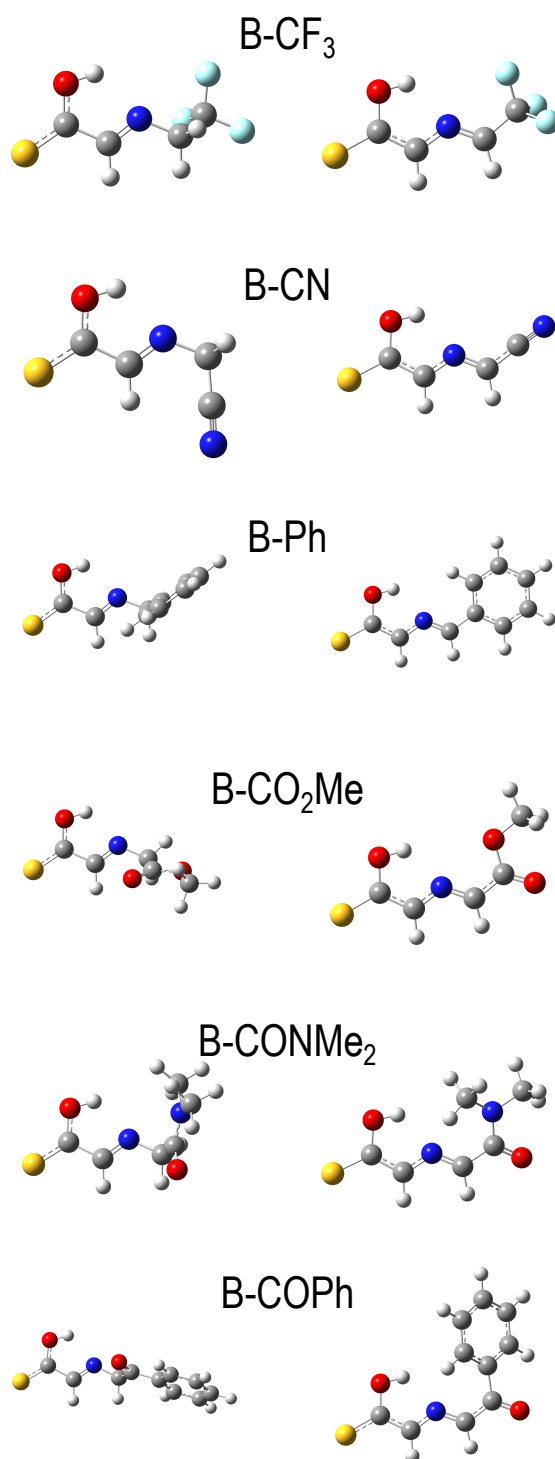


**Figure 3:** Most stable isomers of molecular structure **B** with the different EWG studied (see Fig.1). Left column neutral structures, right column anionic counterparts.

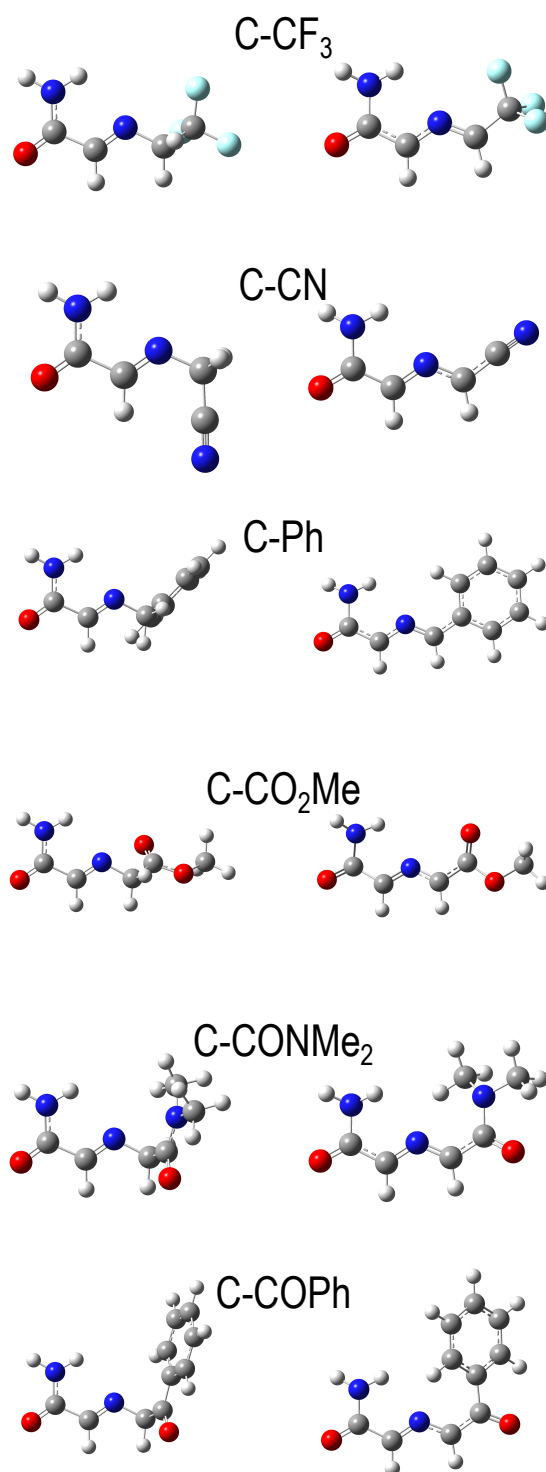


**Figure 4:** Most stable isomers of molecular structure **C** with the different EWG studied (see Fig.1). Left column neutral structures, right column anionic counterparts.

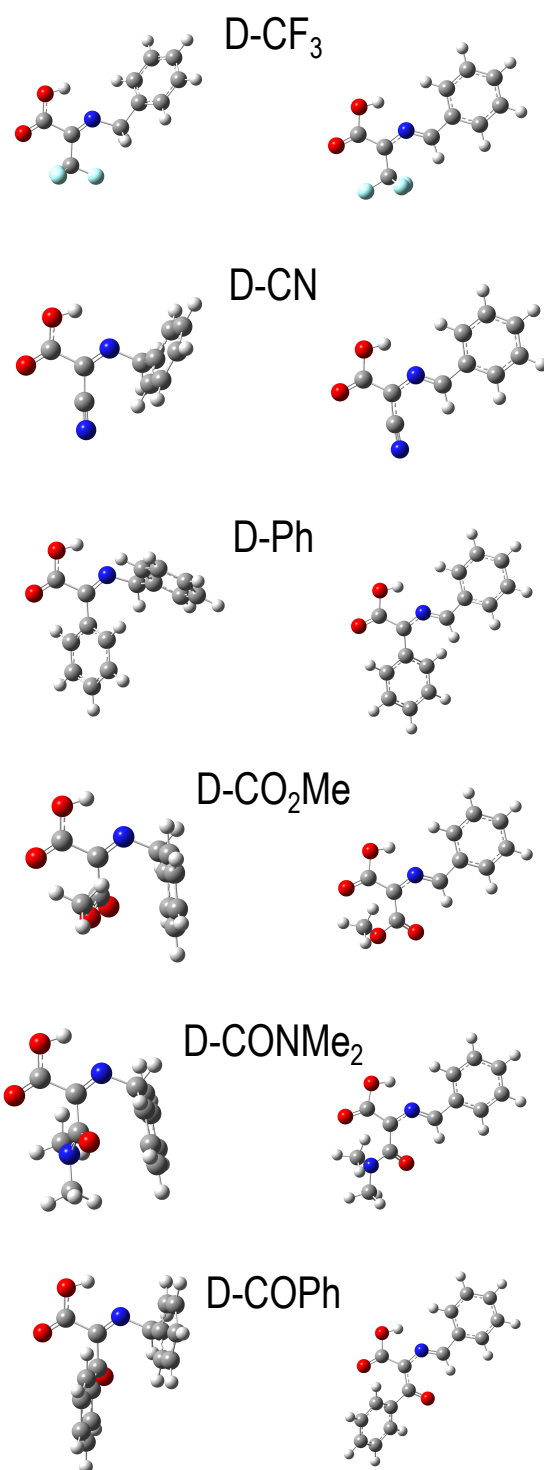


**Figure 5:** Most stable isomers of molecular structure **D** with the different EWG studied (see Fig.1). Left column neutral structures, right column anionic counterparts.

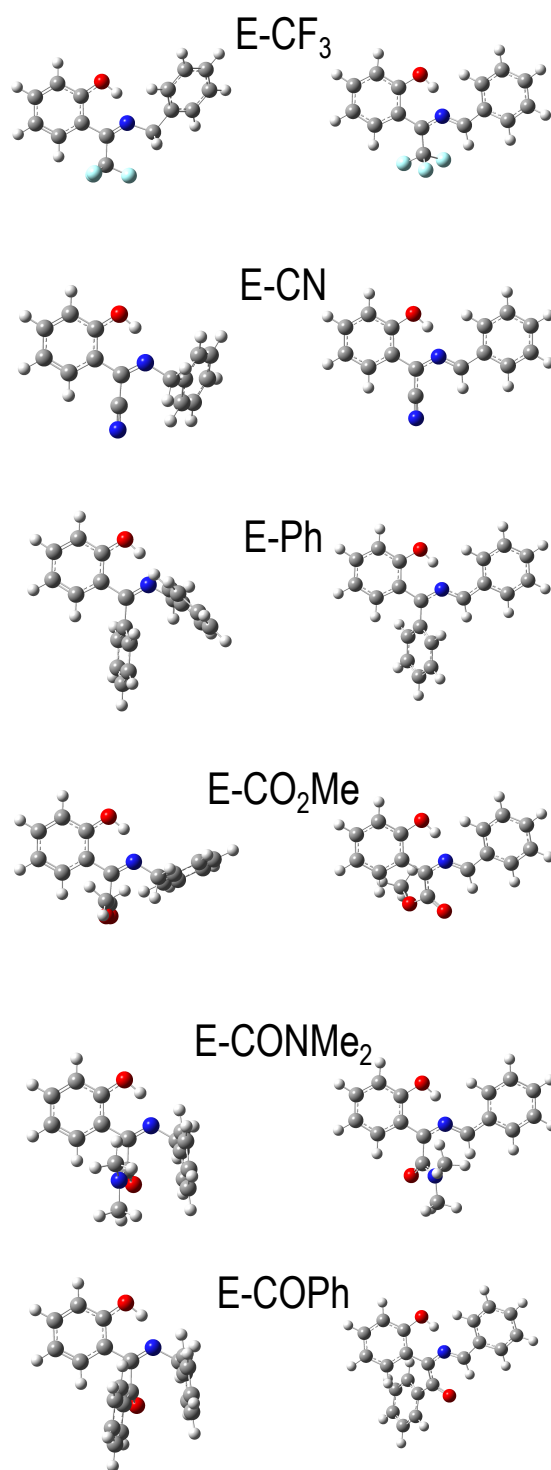


**Figure 6:** Most stable isomers of molecular structure **E** with the different EWG studied (see Fig.1). Left column neutral structures, right column anionic counterparts.

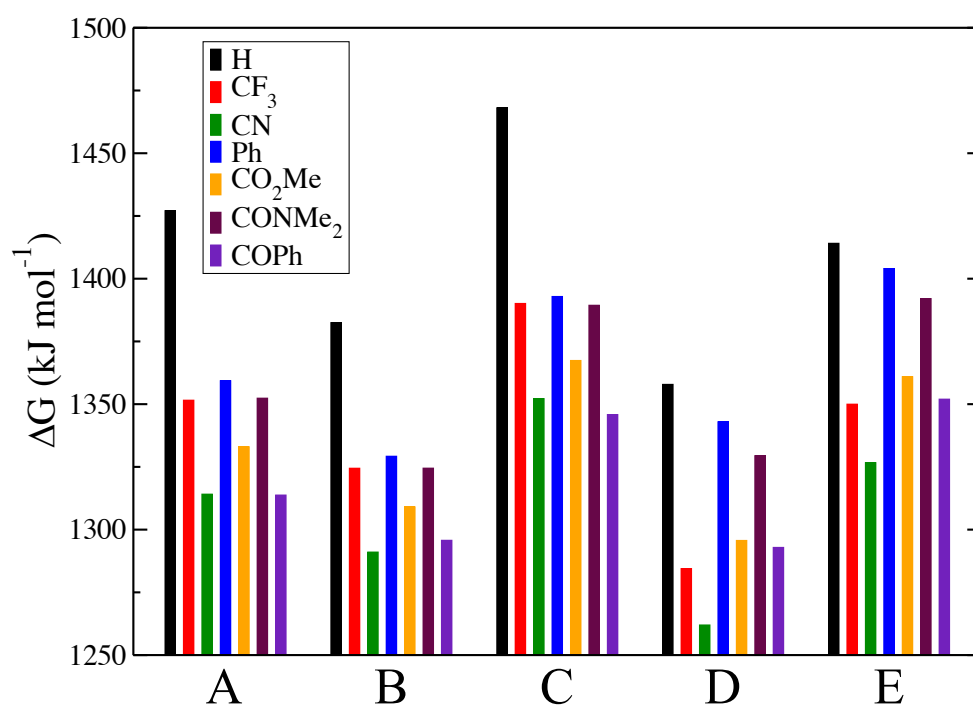


**Figure 7:** Deprotonation Gibbs Free energy  $\Delta G$  (kJ/mol), in the gas phase, for the different species considered in this work.

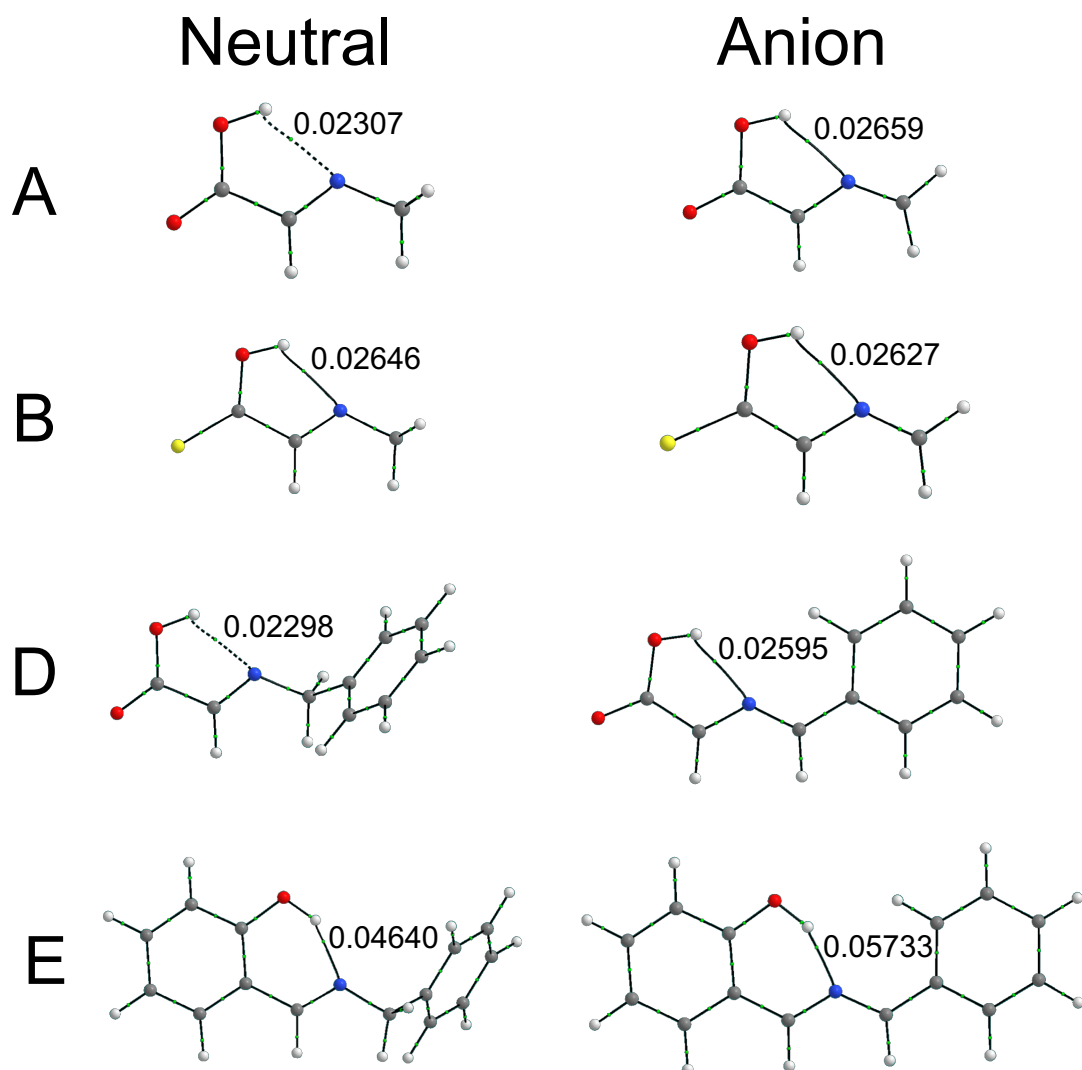


**Figure 8:** Molecular graphs of the neutral and anionic structures **A**, **B**, **D** and **E** (without EWG) showing bond paths (lines), bond critical points (green points) and the electron density (in atomic units:  $e \cdot \text{bohr}^{-3}$ ) in the bond critical point of the intramolecular hydrogen bond.

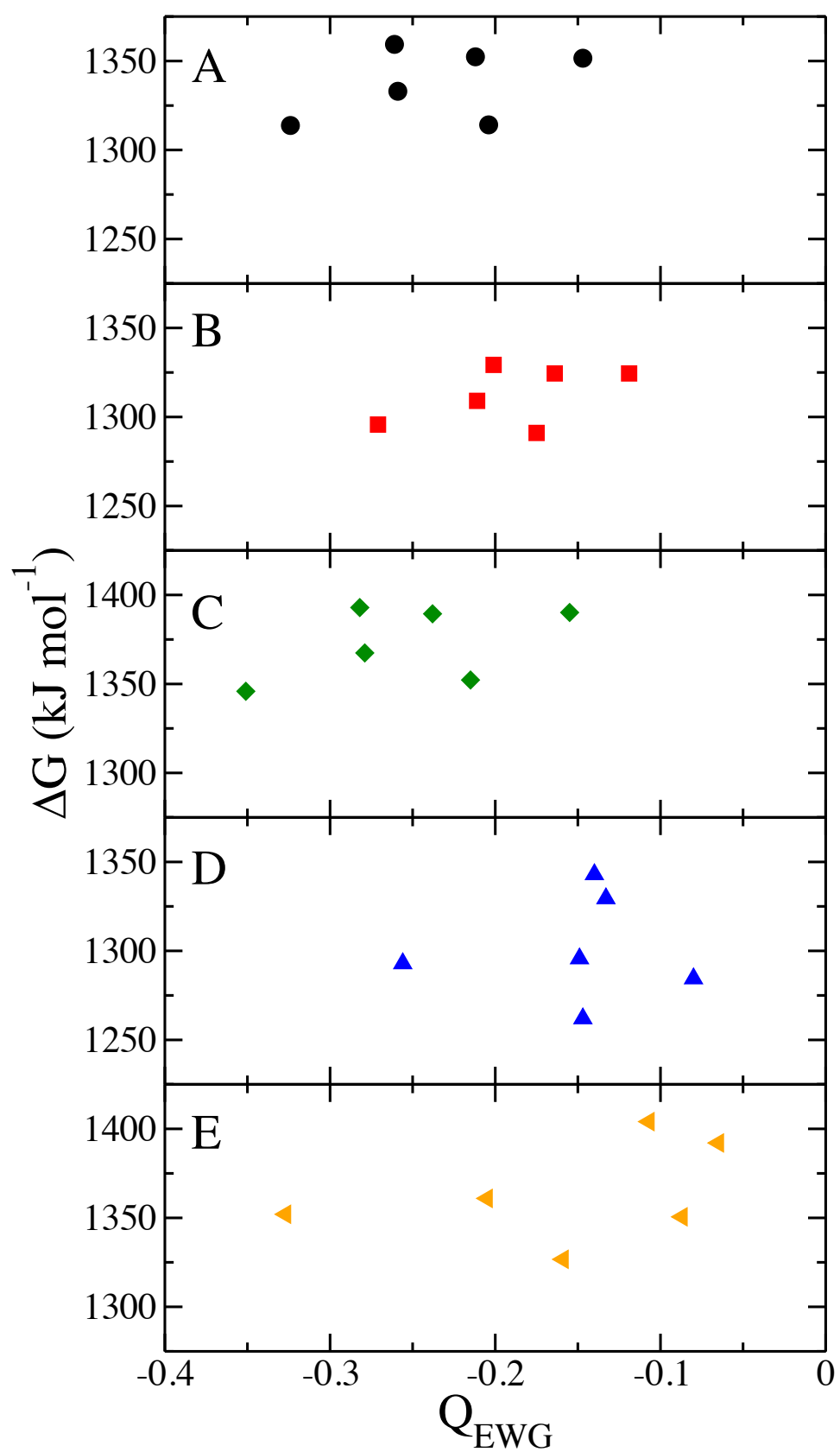


**Figure 9:** Deprotonation Gibbs Free Energy as a function of the charge hosted by the EWG on the anionic structure (after deprotonation).

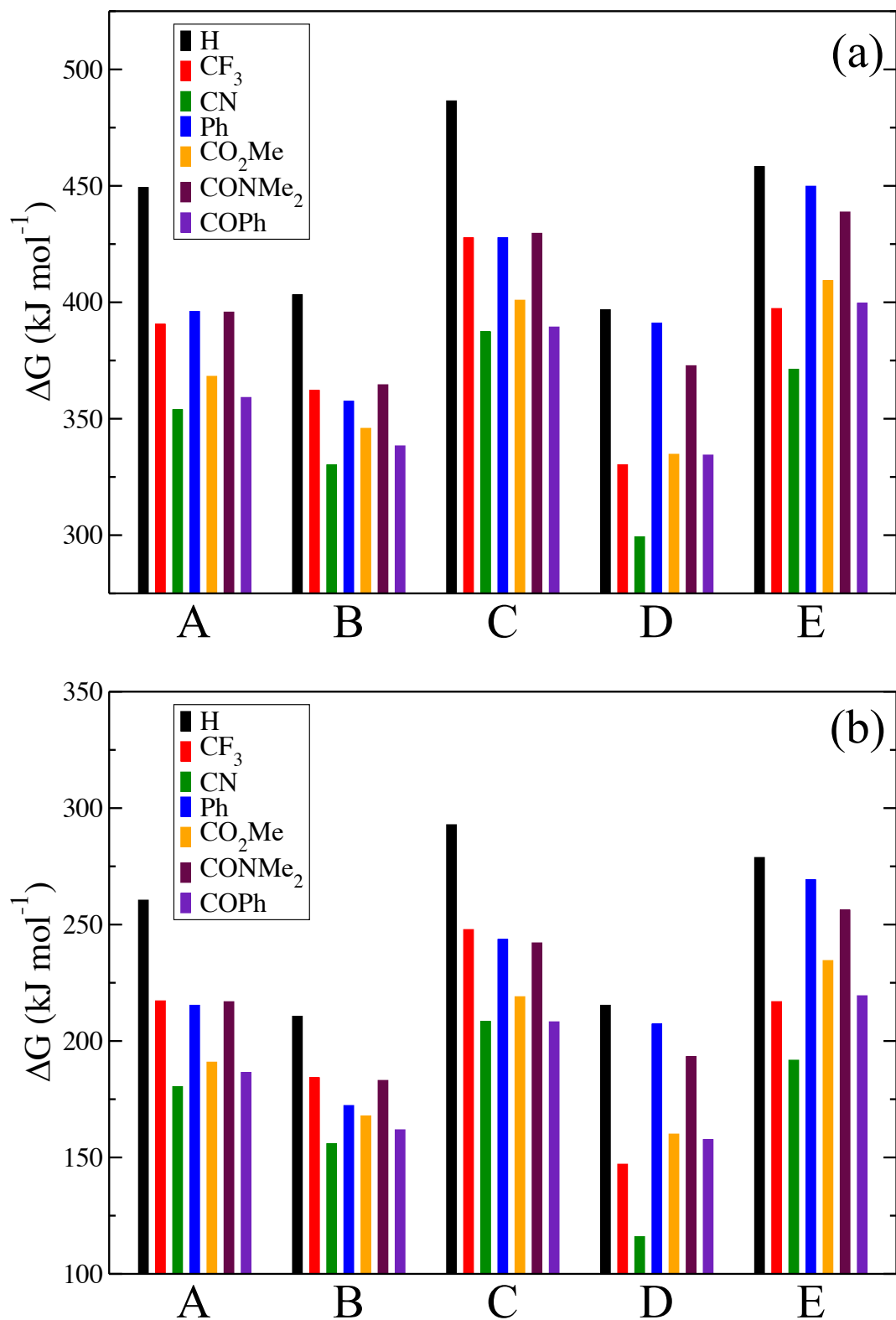
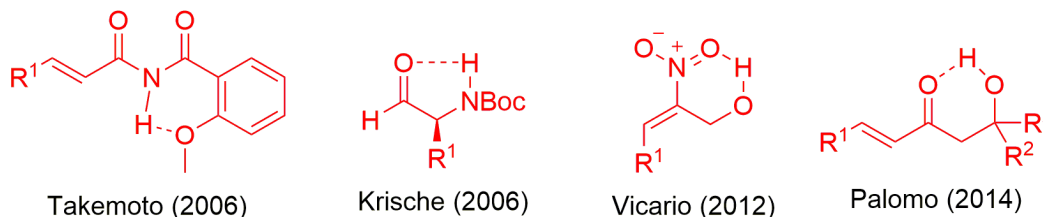


**Figure 10:** Deprotonation Gibbs Free energy  $\Delta G$  ( $\text{kJ/mol}$ ), including solvent effects (a) *p*-xylene and (b) THF, for the different species considered in this work.

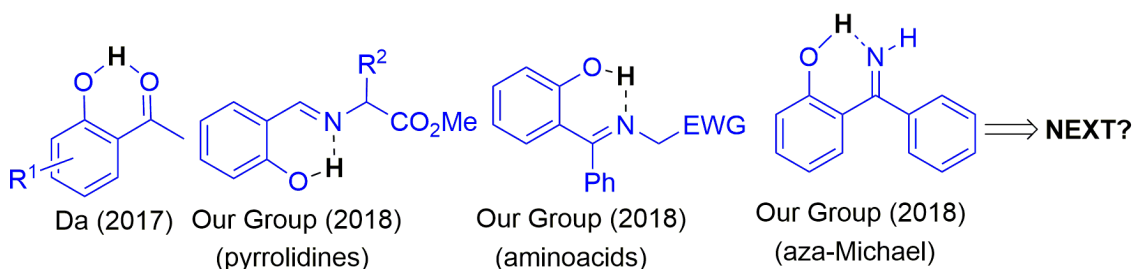


**Scheme 1:** Previous works in the intramolecular hydrogen bond activation of electrophiles (A) and nucleophiles (B) in catalysis.

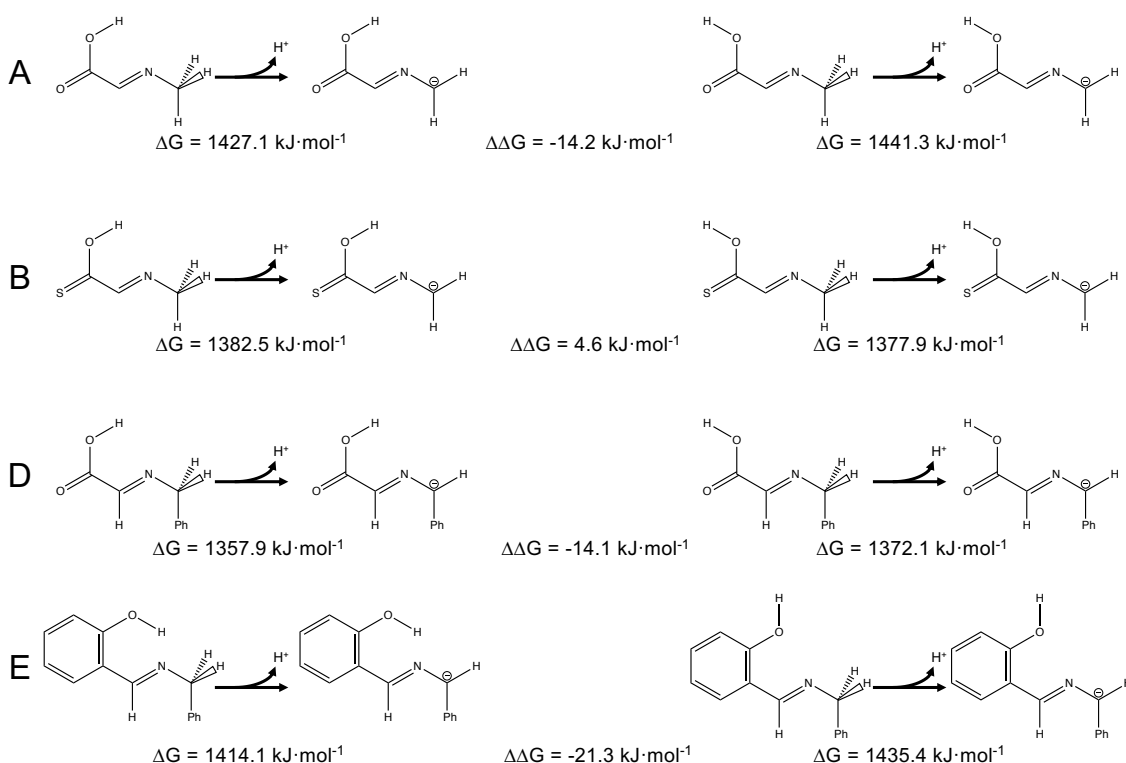
**A-Intramolecular Hydrogen-Bond Activation of electrophiles in Catalysis**



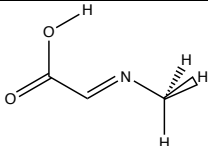
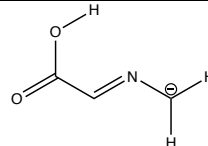
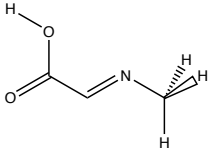
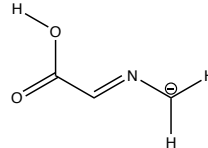
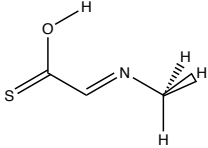
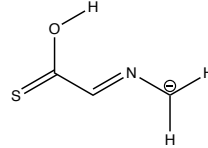
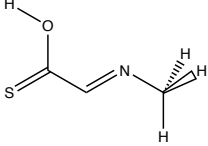
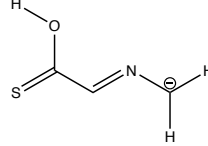
**B-Intramolecular Hydrogen-Bond Activation of nucleophiles in Catalysis**



**Scheme 2:** Deprotonation Gibbs Free Energy ( $\Delta G$ ) for structures **A**, **B**, **D** and **E** without EWG, with and without intramolecular hydrogen bond. The difference between them is also shown ( $\Delta\Delta G$ ).

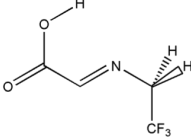
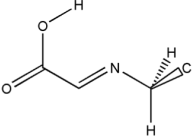
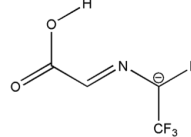
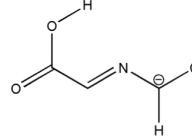
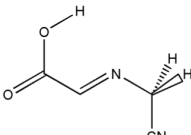
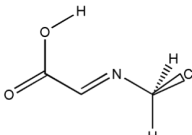
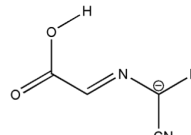
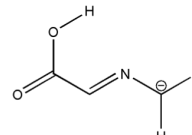
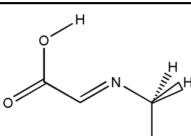
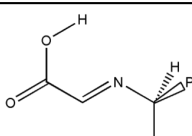
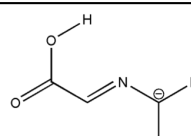
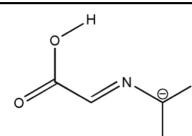
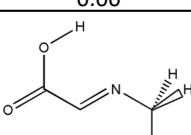
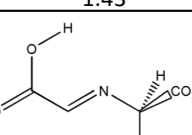
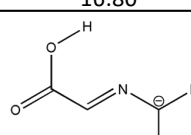
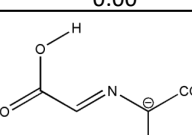
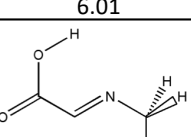
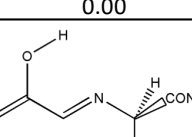
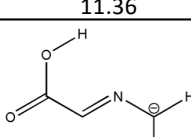
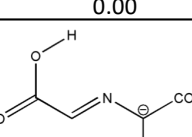
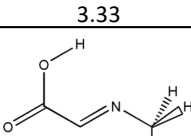
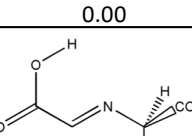
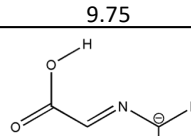
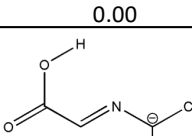


**Table 1.** O-H stretching mode frequency  $\nu_{\text{OH}}$  (in  $\text{cm}^{-1}$ ) of the base structures **A** and **B** without EWG, with and without intramolecular hydrogen bond.

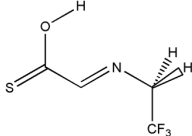
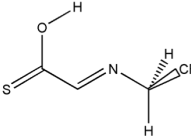
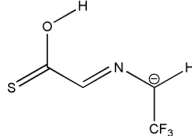
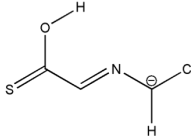
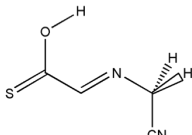
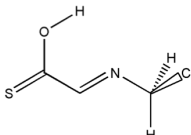
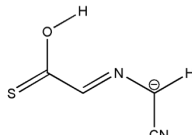
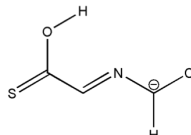
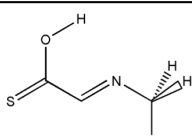
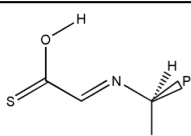
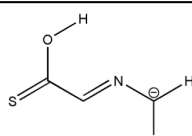
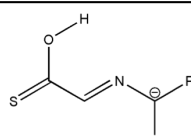
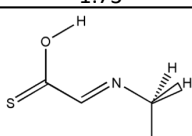
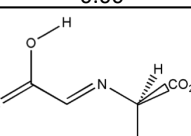
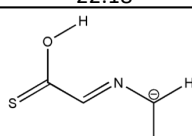
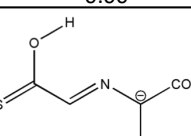
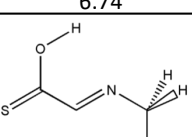
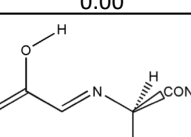
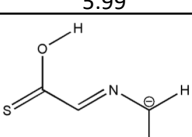
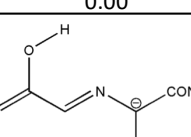
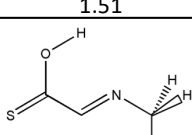
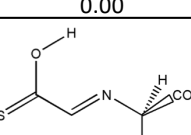
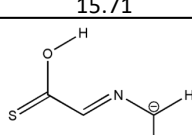
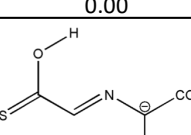
<b>A</b>	Neutral	Anion	Change
H-Bond	 $\nu_{\text{OH}} = 3706 \text{ cm}^{-1}$	 $\nu_{\text{OH}} = 3704 \text{ cm}^{-1}$	-2
No H-Bond	 $\nu_{\text{OH}} = 3830 \text{ cm}^{-1}$	 $\nu_{\text{OH}} = 3864 \text{ cm}^{-1}$	34
<b>B</b>	Neutral	Anion	Change
H-Bond	 $\nu_{\text{OH}} = 3624 \text{ cm}^{-1}$	 $\nu_{\text{OH}} = 3667 \text{ cm}^{-1}$	43
No H-Bond	 $\nu_{\text{OH}} = 3805 \text{ cm}^{-1}$	 $\nu_{\text{OH}} = 3836 \text{ cm}^{-1}$	31

## Appendix

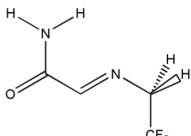
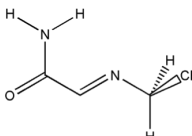
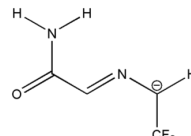
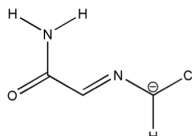
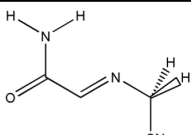
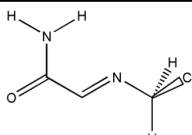
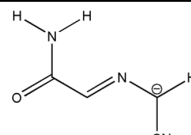
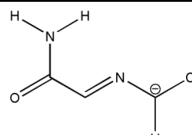
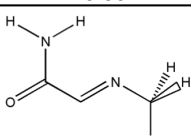
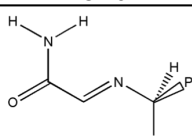
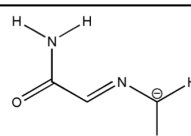
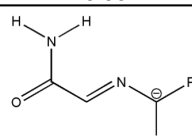
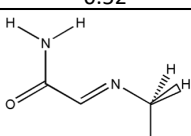
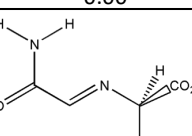
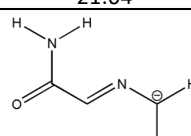
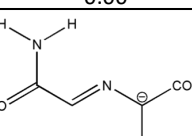
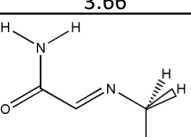
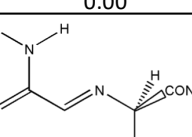
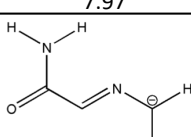
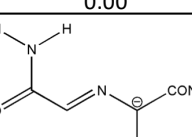
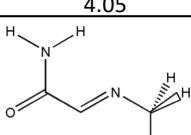
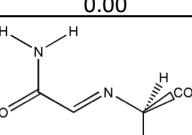
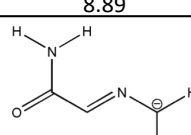
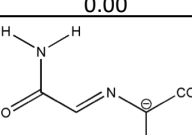
**Table A.** Neutral and anionic conformers of the studied molecules with structure **A** with the different electron withdrawing groups considered. Relative energies are given in  $\text{kJ}\cdot\text{mol}^{-1}$ .

<b>A</b>	<b>Neutral</b>		<b>Anion</b>	
	Conformer 1	Conformer 2	Conformer 1	Conformer 2
<b>CF<sub>3</sub></b>	 5.37	 0.00	 8.36	 0.00
<b>CN</b>	 0.00	 6.83	 2.57	 0.00
<b>Ph</b>	 0.00	 1.43	 16.80	 0.00
<b>CO<sub>2</sub>Me</b>	 6.01	 0.00	 11.36	 0.00
<b>CONMe<sub>2</sub></b>	 3.33	 0.00	 9.75	 0.00
<b>COPh</b>	 5.40	 0.00	 7.75	 0.00

**Table B.** Neutral and anionic conformers of the studied molecules with structure **B** with the different electron withdrawing groups considered. Relative energies are given in  $\text{kJ}\cdot\text{mol}^{-1}$ .

<b>B</b>	<b>Neutral</b>		<b>Anion</b>	
	Conformer 1	Conformer 2	Conformer 1	Conformer 2
<b>CF<sub>3</sub></b>	 6.16	 0.00	 11.77	 0.00
<b>CN</b>	 0.00	 6.39	 4.17	 0.00
<b>Ph</b>	 1.73	 0.00	 22.18	 0.00
<b>CO<sub>2</sub>Me</b>	 6.74	 0.00	 5.99	 0.00
<b>CONMe<sub>2</sub></b>	 1.51	 0.00	 15.71	 0.00
<b>COPh</b>	 7.77	 0.00	 13.05	 0.00

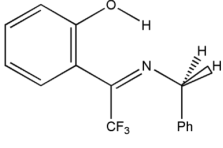
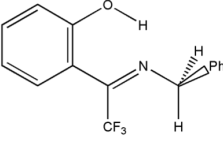
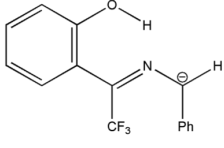
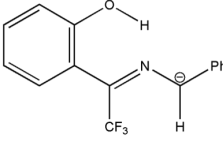
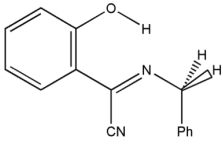
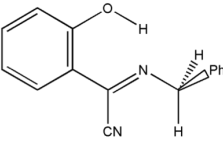
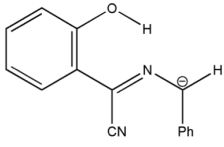
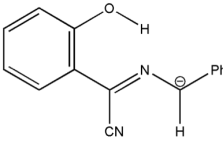
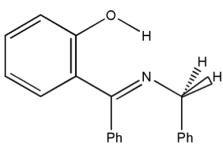
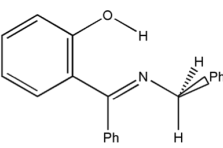
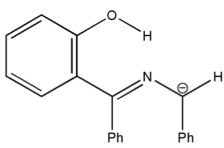
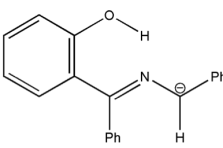
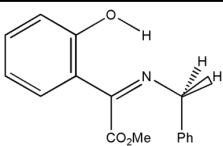
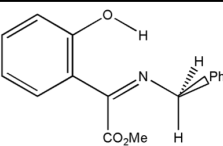
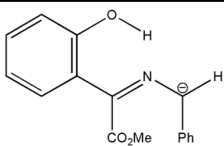
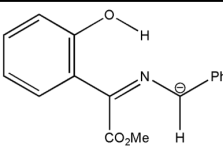
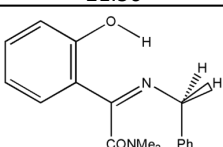
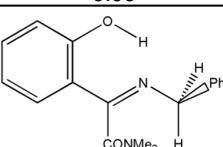
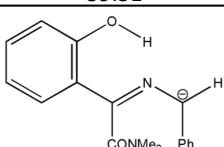
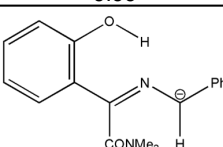
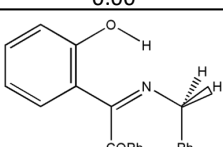
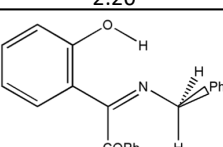
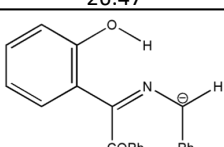
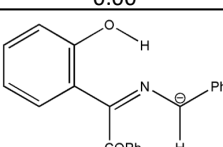
**Table C.** Neutral and anionic conformers of the studied molecules with structure **C** with the different electron withdrawing groups considered. Relative energies are given in  $\text{kJ}\cdot\text{mol}^{-1}$ .

<b>C</b>	<b>Neutral</b>		<b>Anion</b>	
	Conformer 1	Conformer 2	Conformer 1	Conformer 2
<b>CF<sub>3</sub></b>	 5.99	 0.00	 10.35	 0.00
<b>CN</b>	 0.00	 5.76	 4.42	 0.00
<b>Ph</b>	 0.52	 0.00	 21.04	 0.00
<b>CO<sub>2</sub>Me</b>	 3.66	 0.00	 7.97	 0.00
<b>CONMe<sub>2</sub></b>	 4.05	 0.00	 8.89	 0.00
<b>COPh</b>	 7.69	 0.00	 12.92	 0.00

**Table D.** Neutral and anionic conformers of the studied molecules with structure **D** with the different electron withdrawing groups considered. Relative energies are given in  $\text{kJ}\cdot\text{mol}^{-1}$ .

<b>D</b>	<b>Neutral</b>		<b>Anion</b>	
	Conformer 1	Conformer 2	Conformer 1	Conformer 2
<b>CF<sub>3</sub></b>	 3.70	 0.00	 47.84	 0.00
<b>CN</b>	 13.20	 0.00	 39.61	 0.00
<b>Ph</b>	 5.20	 0.00	 30.17	 0.00
<b>CO<sub>2</sub>Me</b>	 0.00	 4.77	 39.16	 0.00
<b>CONMe<sub>2</sub></b>	 0.00	 0.97	 35.43	 0.00
<b>COPh</b>	 2.35	 0.00	 40.22	 0.00

**Table E.** Neutral and anionic conformers of the studied molecules with structure **E** with the different electron withdrawing groups considered. Relative energies are given in  $\text{kJ}\cdot\text{mol}^{-1}$ .

<b>E</b>	<b>Neutral</b>		<b>Anion</b>	
	Conformer 1	Conformer 2	Conformer 1	Conformer 2
<b>CF<sub>3</sub></b>	 5.68	 0.00	 40.27	 0.00
<b>CN</b>	 17.35	 0.00	 41.48	 0.00
<b>Ph</b>	 5.07	 0.00	 34.86	 0.00
<b>CO<sub>2</sub>Me</b>	 21.56	 0.00	 39.31	 0.00
<b>CONMe<sub>2</sub></b>	 0.00	 2.20	 26.47	 0.00
<b>COPh</b>	 0.00	 3.08	 39.76	 0.00